Fez function is required to maintain the size of animal plate in the sea urchin embryo

Shunsuke Yaguchi[a,b,*], Junko Yaguchi[a,b], Zheng Wei[c], Yinhua Jin[a], Lynne M. Angerer[c], Kazuo Inaba[a]

[a]Shimoda Marine Research Center, University of Tsukuba, 5-10-1 Shimoda, Shizuoka 415-0025, Japan

[b]Initiative for the Promotion of Young Scientists' Independent Research, University of Tsukuba, 5-10-1 Shimoda, Shizuoka 415-0025, Japan

[c]Developmental Mechanisms Section, National Institute of Dental and Craniofacial Research, National Institutes of Health, 30 Convent Dr. MSC 4326, Bethesda, MD 20892, USA

Running title: Fez establishes neural border
Key words: BMP, cell fate specification, body axis, neurogenesis

*Corresponding Author: Shunsuke Yaguchi, Shimoda Marine Research Center, University of Tsukuba, 5-10-1, Shimoda, Shizuoka, Japan 415-0025
Phone; +81-558-22-6716
Fax; +81-558-22-0346
E-mail; yag@kurofune.shimoda.tsukuba.ac.jp

Summary

Partitioning ectoderm precisely into neurogenic and non-neurogenic regions is an essential step for neurogenesis of almost all bilaterian embryos. Although it is widely accepted that the antagonism between BMP and its inhibitors primarily sets up the border between these two types of ectoderm, it is unclear how such extracellular, diffusible molecules create a sharp and precise border at the single-cell level. Here, we show that Fez, a zinc finger protein, functions as an intracellular factor attenuating BMP signaling specifically within the neurogenic region at the anterior end of sea urchin embryos, termed the animal plate. When Fez function is blocked, the size of this neurogenic ectoderm becomes smaller than normal. However, this reduction is rescued in Fez morphants simply by blocking BMP2/4 translation, indicating that Fez maintains the size of the animal plate by attenuating BMP2/4 function. Consistent with this, the gradient of BMP activity along the aboral side of the animal plate, as measured by pSmad1/5/8 levels, drops significantly in cells expressing Fez and this steep decline requires Fez function. Our data reveal that this neurogenic ectoderm produces an intrinsic system that attenuates BMP signaling to ensure the establishment of a stable, well-defined neural territory, the animal plate.

Introduction

Nervous system development in bilaterians is composed of a number of developmental processes, such as partitioning the ectoderm into neuroectoderm and non-neuroectoderm, patterning the neuroectoderm, and differentiation of neural cells including neural network formation. Among these, partitioning of ectoderm is one of the earliest and the most critical events because all of the following processes of neurogenesis depend on it. In vertebrates, the prospective neuroectoderm is formed at the future dorsal side by the function of the Spemann organizer, which can induce an ectopic neuroectoderm when grafted to the ventral region of the embryo (Spemann and Mangold, 1924). From a number of previous studies analyzing the inductive function of the organizer, we now know the molecular entities mediating this induction are diffusible extracellular molecules such as Chordin, Noggin, and Follistatin (De Robertis and Kuroda, 2004). These molecules antagonize the function of BMP, a member of TGF-ß superfamily, on the dorsal side protecting this region from BMP-mediated induction of non-neuroectoderm (Khokha et al., 2005). When one or two of them are knocked down,

the neuroectoderm is normally partitioned and the morphants have normal neural cell differentiation. However, when the expression of all three is knocked down, the embryo contains no neuroectoderm because of enhanced and expanded BMP signaling. Conversely, when the translation of three BMP members (2, 4, and 7) is blocked, the embryo has expanded neuroectoderm (Reversade et al., 2005). Therefore, it is widely accepted that protection against BMP activity is the mechanism that specifies the dorsal region as neuroectoderm during early development in vertebrates (De Robertis and Kuroda, 2004). However, BMPs are diffusible extracellular molecules that form an activity gradient that is reinforced by positive feedback (Reversade and De Robertis, 2005; Shen et al., 2007), such that a small initial change can have a large influence on the effective signaling range (Gardner et al., 2000). Therefore, it has been unclear how BMP activity can be precisely controlled to partition ectoderm fates at a single-cell level. Because the size of the neuroectoderm is identical in individual embryos of the same species at the same developmental stage, there must be additional intrinsic mechanism(s) that down regulate BMP signaling and establish precise domains of neural and non-neural ectoderm.

The neurogenic ectoderm of the embryo of the sea urchin, a basal deuterostome, consists of two major parts. One is the ectoderm at the animal pole that is highly related to the vertebrate anterior neuroectoderm, judged from the temporal and spatial expression patterns of genes encoding regulatory factors, and from the fact that canonical Wnt signaling is involved in positioning the region anteriorly during cell-fate specification at early embryogenesis (Wikramanayake et al., 1998; Kiecker and Niehrs, 2001; Wei et al., 2009). The second forms within the ciliary band located at the border between oral and aboral signaling territories (Duboc et al., 2004; Yaguchi et al., 2006; Wei et al., 2009; Lapraz et al., 2009; Yaguchi et al., 2010a; Saudemont et al., 2010). The anterior neurogenic region, called the animal plate is the focus of the present study. FoxQ2 is among several genes that are the earliest to be specifically expressed in neurogenic ectoderm. FoxQ2 transcripts appear in the entire animal half at 32-cell stage and are progressively restricted to the animal pole region in pre-hatching blastulae (Tu et al., 2006; Yaguchi et al., 2008). This process restricts at least several genes required for animal plate development and depends on the Wnt/ß-catenin pathway, which functions in the vegetal hemisphere (Logan et al., 1999; Yaguchi et al., 2008). After the restriction of FoxQ2-positive region is completed at the blastula stage, the prospective neuroectoderm starts to express additional genes specific for nervous system development (Wei et al.,

2009). However, at around this stage, *nodal* and *bmp2/4*, which are common anti-neural factors during early development, are transcribed on the oral side and then, BMP2/4 diffuses to the aboral ectoderm. Both Nodal and BMP2/4 induce non-neurogenic ectoderm fates (Angerer et al., 2000; Duboc et al., 2004; Bradham et al., 2009; Lapraz et al., 2009; Saudemont et al., 2010). The prospective animal plate, as well as ciliary band, neuroectoderm must have robust mechanisms that antagonize these signals and maintain their precise sizes during these stages. Here, we report that, in the animal plate, FoxQ2 induces production of an intracellular transcription factor, Fez (forebrain embryonic zinc finger), at blastula stage that specifically attenuates BMP signaling, thereby maintaining and stabilizing the border of the anterior neuroectoderm in the sea urchin embryo.

Materials and Methods

Animals and embryo culture

Adult sea urchins, *Strongylocentrotus purpuratus*, were obtained from The Cultured Abalone, Goleta, CA, and the embryos were used only for the microarray experiment. For all other experiments, embryos of *Hemicentrotus pulcherrimus* collected around Shimoda Marine Research Center, University of Tsukuba, and around Marine and Coastal Research Center, Ochanomizu University were used. The gametes were collected by intrablastocoelar injection of 0.5 M KCl and the embryos were cultured by standard methods with filtered natural seawater (FSW) at 15 ˚C. For some experiments, gamma-secretase inhibitor (DAPT; Sigma-Aldrich, St. Louis, MO, USA) was added at hatching blastula stage to a final concentration of 20 μM.

Microarray

Sample preparation, microarray, and data processing were described previously (Wei et al., 2006). The double-strand cDNAs synthesized from control embryos and SpFoxQ2 morphants were labeled, hybridized, and scanned by Roche Nimblegen microarray services. The microarray was prepared based on *S. purpuratus* genome sequence information (Wei et al., 2006; Sea Urchin Genome Sequencing Consortium, 2006) and hybridized with amplified cDNAs isolated from *S. purpuratus* mesenchyme blastulae either containing or lacking SpFoxQ2-MO1 previously described (Yaguchi et al., 2008; see below). FoxQ2-dependent genes identified in the microarray were confirmed by *in situ* hybridization in *H. pulcherrimus* embryos, as described below and by quantitative polymerase chain reaction (QPCR) as previously described (Yaguchi et al.,

2010b).

Microinjection of morpholino antisense oligonucleotides (MO) and synthetic mRNAs

Microinjection was performed as described previously (Yaguchi et al., 2010b). We used the following morpholinos (Gene Tools, Philomath, OR, USA) at the indicated concentrations in 24% glycerol in injection needles: SpFoxQ2-MO1 (800 µM; Yaguchi et al., 2008), FoxQ2-MO (200 µM; Yaguchi et al., 2010b), Fez-MO1 (1.9 mM), Fez-MO2 (1.6 mM), BMP2/4-MO (400 µM), Smad1/5/8-MO (1.0 mM). All morpholinos were designed against *H. pulcherrimus* genes except for the SpFoxQ2-MO1 that blocks *S. purpuratus* FoxQ2 translation. The morphant phenotypes were the same as those previously published (Duboc et al., 2004; Yaguchi et al., 2008). The morpholino sequences were the following:

Fez-MO1: 5'- GAATGCTTTTTTCATGCACTAAAGA-3',
Fez-MO2: 5'- GCGTTCAAATCTACTTAAGGAGTGT-3',
BMP2/4-MO: 5'-GACCCCAATGTGAGGTGGTAACCAT-3', and
Smad1/5/8-MO: 5'- GCCATCGACATAGTGGAGCAAGCTT-3'.

mRNAs were synthesized from linearized plasmids using the mMessage mMachine kit (Life Technologies, Carlsbad, CA, USA), and injected at the indicated concentrations in 24% glycerol in injection needles: Δ-cadherin (0.3-0.6 µg/µl; Logan et al., 1999), Fez-mRNA (2.0 µg/µl), BMP2/4-mRNA (2.5 µg/µl), actSmad2/3-mRNA (2.5 µg/µl; Yaguchi et al., 2007).

Whole-mount *in situ* hybridization and immunohistochemistry

Whole-mount *in situ* hybridization was performed as described previously (Minokawa et al., 2004; Yaguchi et al., 2010b). The *foxQ2*-positive cell number for the experiment in Figure 5 was determined by counting DAPI signals in the *foxQ2* region through serial optical sections. Immunohistochemistry for detecting serotonin, synaptotagminB (synB), and Nk2.1 was performed as described previously (Yaguchi et al., 2006). To detect FoxQ2 and pSmad1/5/8 immunochemically, embryos were fixed with 4% paraformaldehyde-FSW for 10 min. After washing with phosphate-buffered saline containing 0.5% Tween-20 (PBS-T) five times, the embryos were blocked with 1% skim milk (Difco; BD, Franklin Lakes, NJ, USA) in PBS-T and incubated with primary antibodies diluted as follows with Can Get Signal immunostain solution B (TOYOBO,

Tokyo, Japan):
mouse anti-FoxQ2 IgG 1:100,
rabbit anti-pSmad1/5/8 (Cell Signaling Technology #9511; Danvers, MA, USA) 1:1000. The primary antibodies were detected with secondary antibodies conjugated with Alexa-568 for FoxQ2 and Alexa-488 for pSmad1/5/8 (Life Technologies). The specimens were observed with a Zeiss Axio Imager.Z1 equipped with Apotome system, and optical sections were stacked and analyzed with ImageJ and Adobe Photoshop. Panels and drawings for figures were made with CANVAS software.

Anti-FoxQ2 antibody preparation

cDNA encoding full-length FoxQ2 was cloned into the pET vector (Novagen, Darmstadt, Germany) and histidine-tagged FoxQ2 was induced in bacteria with IPTG. The bacteria were lysed with 6 M Urea, and the fusion protein was purified by Ni-column chromatography and used to immunize three mice. Antisera were screened by whole-mount immunohistochemistry, and IgG was purified with Melon gel (Thermo Fisher Scientific, Waltham, MA, USA).

Results

***Fez* expression depends strongly on FoxQ2 during blastula stages.**

FoxQ2 is expressed very early in the prospective animal plate of sea urchin embryos and is required for the development of neurons in this region of the embryonic nervous system. We searched for regulatory genes downstream of FoxQ2 required for formation of the animal plate using a microarray approach to identify genes strongly down regulated in FoxQ2 morphants at the blastula stage of *Strongylocentrotus purpuratus*. Previous studies have shown this approach to be successful in identifying genes whose expression depends on upstream regulatory proteins (Wei et al., 2009; Yaguchi et al., 2010b). One candidate FoxQ2-dependent regulatory gene encoded an apparent ortholog of Fez, forebrain embryonic zinc finger, (SPU_027491; Sea Urchin Genome Sequencing Consortium, 2006). We recovered this gene from the genome of the Japanese sea urchin, *Hemicentrotus pulcherrimus*, and found that it contains sequences encoding an engrailed homology repressor motif 1 (EH1) at the N-terminal region and six zinc finger domains at C-terminus (accession number; AB610478), as previously reported for vertebrate Fez or Fez-like proteins (e.g. mice; AK014242 and AB042399, Hirata et al., 2006b). Because of its containing EH1, Fez is thought to

function as a transcriptional repressor (Hirata et al., 2006a). After confirming the microarray result that, during blastula stages, *H. pulcherrimus* FoxQ2 morphants have significantly decreased *fez* mRNA levels by *in situ* hybridization and QPCR (Fig. 1M-O), we focused on the function of Fez in neurogenesis.

Expression of *fez* during development

To examine the gene expression pattern of *fez*, we performed *in situ* hybridization at stages from egg to pluteus larva. No signals were detected before hatching (Fig. 1A), consistent with the temporal profiling data conducted by Wei et al., (2006) using microarrays. After hatching, *fez* transcripts accumulate throughout the entire animal plate (Fig, 1B) until early gastrula stage (Fig. 1C). After the embryo reaches mid-gastrula stage, the uniform expression fades and is progressively replaced by stronger signals in a few individual cells within the animal plate (Fig. 1D-F, asterisks). To compare *fez* and *foxQ2* expression patterns in detail, we employed fluorescent *in situ* hybridization. *fez* is expressed at low levels in the animal plate at hatching blastula stage (Fig. 1G) but much stronger at mesenchyme blastula stage and in a pattern that is almost identical to that of *foxQ2* (Fig. 1H). As shown with chromogenic detection (Fig. 1D), *fez* transcripts accumulate in individual cells at gastrula stage, whereas *foxQ2* expression remains uniform throughout the animal plate (Fig. 1I, J). The expression domain of *foxQ2* is restricted to the oral side of the animal plate at later stages (Yaguchi et al., 2008) whereas 3-5 individual *fez*-positive cells are located on the opposite (aboral) side at that time (Fig. 1K; insets in Fig. 1I'', J'', K''). To examine which cell type(s) express *fez* mRNA, we compared the distributions of *tryptophan 5-hydroxylase* (*tph*) and *fez* mRNAs by double fluorescent *in situ* hybridization. Because TPH is the rate-limiting enzyme in serotonin synthesis, it is a specific marker for serotonergic neurons in sea urchin embryos (Yaguchi and Katow, 2003). At the prism stage, *fez* is clearly expressed in the serotonergic neurons although each mRNA localizes to a slightly different position in the same cell (Fig. 1L). Because the expressions of *fez* and *foxQ2* do not overlap at later stages *fez* expression does not depend on FoxQ2 at that time (Fig. 1O). In summary, *fez* is expressed throughout the animal plate between hatching blastula and gastrula stages, and in serotonergic neural precursors and neurons after gastrulation.

Fez controls the size of the animal plate.

To examine Fez function in sea urchin development and neurogenesis, we

performed knockdown and mis-expression experiments by injecting morpholino anti-sense oligonucleotides (MO) and mRNA encoding full-length Fez protein, respectively. In Fez morphants, the timing of cleavage and invagination is slightly delayed but otherwise no morphological defects are detectable (data not shown). However, Fez morphants have fewer serotonergic neurons than do normal embryos and the region in which they differentiate is smaller, being restricted to an area between the bases of anterolateral arms at the 72-hour pluteus stage (Fig. 2B). In contrast, in normal embryos, the left and right borders of the serotonergic neural complex extend up to the middle of those arms (Fig. 2A). This phenotype is specific because it was also obtained with a second morpholino targeted to a non-overlapping sequence in the mRNA (Fig. S1). Because the cell bodies and axon network of synaptotagminB-positive, non-serotonergic neurons beneath the ciliary band in Fez morphants are almost identical to those of normal embryos (*cf.* Fig. 2B' with 2A'; Nakajima et al., 2004; Burke et al., 2006), the loss of Fez function likely affects only the serotonergic neurons on the aboral side of the animal plate. There are two possibilities for the decreased number of serotonergic neurons in Fez morphants. One is that the animal plate itself becomes smaller than that of normal embryos, and another is that the size of animal plate is same but the differentiation of serotonergic neurons is perturbed at the periphery of this region. To test this, we focused on the position of the first pair of serotonergic neurons that develop near the aboral-lateral margins of the animal plate, which is marked with Nk2.1 expression (Fig. 2D, F; Yaguchi et al., 2000: Yaguchi et al., 2006). Although Fez morphants have fewer serotonergic neurons than do control embryos at later stages (Fig. 2A, B), the timing of the differentiation of the first pair of serotonergic neurons is same. In Fez morphants, these serotonergic neurons are closer to each other than those in normal embryo, and there are fewer Nk2.1-positive cells between them (Fig. 2D', F'). Here the serotonergic neurons are stained with anti-SynB antibody because at this stage all SynB neurons are serotonergic. In addition, the expression of *homeobrain* (*hbn*) suggests that the animal plate is smaller. *hbn* expression is cleared from the animal plate and surrounds it at gastrula and pluteus stages (Wei et al., 2009). However, the central region of clearance is smaller in Fez morphants than in controls (*cf.* Fig. 2G with E). Moreover, treatment of embryos with gamma-secretase inhibitor (DAPT), which suppresses Notch signaling, supports these results. In the sea urchin embryos, delta-Notch signaling suppresses differentiation of serotonergic neurons through lateral inhibition (Wei et al., 2011). Thus, if Notch signaling is blocked, additional neural precursors can differentiate and

contribute to a cluster of serotonergic neurons. If the primary function of Fez, whose early expression is in all cells of the animal plate, is to support the differentiation of each as a neuron, then the additional neurons that develop in DAPT-treated embryos (Fig. 3C) would not appear in Fez morphants. However, this is not the case, because the number of neurons increases and they form a cluster in DAPT-treated embryos, regardless of whether Fez is present or absent (Fig. 3A-E). This indicates that Fez is not required just for the differentiation of serotonergic neurons, but rather for determining the size of neurogenic ectoderm. Furthermore, mis-expression of Fez can significantly increase the size of the animal plate and the number of serotonergic neurons, which extend all the way to the tip of anterolateral arms (Fig. 2C, 3F, G). In addition, because the size of neural cluster along the oral-aboral axis in DAPT-treated Fez mRNA-injected embryos is wider than that in control embryos, Fez misexpression can expand the animal plate along both ciliary band and the aboral ectoderm.

Fez maintains the neurogenic ectoderm during blastula stages

The loss-of-function experiments suggest that Fez is required to maintain the size of the neurogenic animal plate in the sea urchin embryo. To investigate when Fez executes this function, we examined the expression patterns of *foxQ2* and its downstream gene, *nk2.1*. *fez* begins to be expressed between hatching and mesenchyme blastula stages in control embryos (Fig. 1), and the size of the animal plate marked by *foxQ2* at both stages is almost identical in control embryos (Fig. 4A, B). The FoxQ2-dependent gene, *nk2.1*, begins to be expressed at mesenchyme blastula stage in a similarly sized region of the neurogenic ectoderm (Fig. 4C). In contrast, in Fez morphants, the size of the *foxQ2*-expressing domain at mesenchyme blastula stage becomes smaller than that at hatching blastula stage (Fig. 4D, E), and significantly smaller than that in control embryos at the mesenchyme blastula stage (*cf.* Fig. 4E with B). As well, the size of the *nk2.1*-expressing region decreases (Fig. 4F). Taken together, these data indicate that Fez is required to maintain the precise size of neurogenic animal plate as soon as it is expressed between hatching and mesenchyme blastula stages.

BMP2/4 can restrict the neurogenic ectoderm

Fez could regulate the size of the animal plate by supporting positive regulators of this domain or by inhibiting negative regulators such as BMP signaling, which suppresses development of other neuroectoderm territories in the sea urchin embryo (Lapraz et al.,

2009; Saudemont et al., 2010; Yaguchi et al., 2010a). To test the first alternative, we employed Δcadherin (Δcad) mRNA-injected embryos that lack Wnt/ß-catenin and TGF-ß signals, and develop a greatly expanded animal plate and flanking region (Logan et al., 1999; Duboc et al., 2004; Yaguchi et al., 2006; Wei et al., 2009). In these embryos, *fez* is expressed throughout the expanded animal plate (Fig. S2). When Fez translation is blocked in Δcadherin (Δcad) mRNA-injected embryos with a Fez morpholino, *foxQ2* expression still covers half or more of the embryo, and its distribution is not distinguishable from that of Δcad only-injected embryos (Fig. S2). This indicates that Fez does not function as an essential feedback inducer of *foxQ2*, an upstream regulator for animal plate development, and suggests the alternative that it functions as an inhibitor of animal plate-repressing signal(s).

To test whether BMP signaling might be the postulated signal that suppresses animal plate development and that is suppressed by Fez, we examined the effects of knocking it down or mis-expressing it throughout the embryo on the expression of *foxQ2* and *fez*. As shown in Figure 4, loss of BMP2/4 does not expand the animal plate or significantly alter the expression of these two genes (Fig. 4G-J), but mis-expression strongly suppresses the expression of both (Fig. 4K, L, arrowhead and double arrowheads). We then asked whether the reduction of the animal plate in Fez morphants, as marked by *foxQ2* expression, requires BMP2/4. To test this, we injected Fez and BMP2/4 morpholinos simultaneously. In Fez morphants in which BMP signaling is normal, the *foxQ2* domain is reduced compared to control embryos (Fig. 4M, N), but not in a double Fez-BMP2/4 morphant (Fig. 4O, P), indicating that in the absence of Fez, BMP signaling changes the size of the animal plate.

Fez protects neurogenic ectoderm against BMP signaling

Although the data strongly suggest that it is BMP2/4 signaling that reduces the animal plate in the absence of Fez, they do not rigorously rule out the possibility that, in the context of Fez-BMP2/4 double morphants, ectopic Nodal, which diffuses to the aboral side of the animal plate (Yaguchi et al., 2010a) might affect its properties or interfere with some other signal that antagonizes the animal plate. To eliminate ectopic Nodal signaling in double morphants from regions where BMP2/4 normally signals, we used an experimental embryo described previously (Yaguchi et al., 2007), in which Nodal signaling is restricted to one side of the embryo. Endogenous Nodal is eliminated with a morpholino injection at the one-cell stage, and Nodal signaling is supplied on only one

side of the embryo by injecting into one blastomere at the two-cell stage mRNA encoding constitutively active Smad2/3 (actSmad2/3) along with mRNA encoding a myc marker. This treatment forces oral and aboral fates on the injected and non-injected sides of the embryo, respectively, because actSmad2/3 activates the oral program that produces BMP2/4 (Fig. S3) that diffuses to and signals to cells on the aboral side and activates the aboral ectoderm program (Yaguchi et al., 2007; Fig. 5A-C). In this embryo, the number of *foxQ2*-positive cells in the aboral half is about 20 (Fig. 5A-C, M; see Materials and Methods), but this number is cut approximately in half in Fez morphants (Fig. 5D-F, M), showing a similar response to that observed between normal and Fez morphants. However, this reduction did not occur in the experimental embryo (doubly injected with Nodal morpholino and actSmad2/3) in which BMP2/4 is also knocked down. The size of neurogenic ectoderm is unchanged in those embryos, whether or not Fez protein is present or absent (Fig. 5G-M). These data indicate that the signal that Fez blocks in the animal plate is BMP2/4. Thus, FoxQ2 causes production of Fez, which attenuates BMP2/4 signaling in the aboral animal plate ectoderm.

To determine if and when BMP2/4 signals in the animal plate, we monitored the presence of phospho-Smad1/5/8 (pSmad1/5/8; Lapraz et al., 2009) and FoxQ2 protein by immunostaining between unhatched blastula and mesenchyme blastula stages. The specificity of each of these antibodies in *H. pulcherrimus* was confirmed because all signals were absent in embryos injected with the corresponding morpholinos (Fig. S4). Furthermore, all pSmad1/5/8 signals at this stage are attributable to BMP2/4 activity, because there are no signals in BMP2/4 morphants (Fig. S4). Before hatching blastula stage, no BMP signaling was detected, but when the embryo hatched, a clear signal appeared in the nuclei of cells in the animal half of the embryo including the animal plate marked by FoxQ2 expression (Fig. 6A, B). However, a few hours later, at mesenchyme blastula stage, BMP2/4 signaling increased dramatically in the future aboral ectoderm and established a decreasing gradient from aboral to oral through animal plate (Fig. 6C; Lapraz et al., 2009). Based on the immunohistochemical data, the relatively strong BMP signaling area is closer to the animal pole in Fez morphants, compared with that in control embryos (Fig. 6D, E). To further analyze this, we measured pixel values on images and used ImageJ software to quantitate relative immuno-fluorescent signal intensities that reflect the relative levels of FoxQ2 and pSmad1/5/8 proteins in nuclei in cells in a line from the animal pole to the center of the aboral side (Fig. 6F, white dots). The data were normalized in each embryo, then averaged among individual batches and shown as

relative intensity. The measurements were performed in 10-14 embryos in three independent batches to check reproducibility. In normal embryos, the concentration of FoxQ2 drops from maximal levels to background in the interval from 3 to 6 cells from the center of the animal plate and within that same interval an inverse relationship exists for pSmad1/5/8 (Fig. 6G, upper panel). A similar inverse relationship exists in Fez morphants, but the corresponding drop in FoxQ2 occurs several cells closer to the center of the animal plate (Fig. 6G, lower panel). In both normal and Fez morphants, maximal levels of FoxQ2 are achieved when pSmad1/5/8 levels are 30-40% of maximal. The clear difference in Fez morphants is that, within the critical region of the animal plate that is defined by half maximal levels of FoxQ2 in control and Fez morphant embryo (vertical dotted dashed lines), the pSmad1/5/8 levels are approximately 20-40% of maximum in controls, but 50-80% of maximum in Fez morphants. Since maximum levels of FoxQ2 and pSmad1/5/8 are the same in control and Fez morphants, and since Fez is not required for FoxQ2 expression, these data indicate that, in this outer region of the animal plate, maximal FoxQ2 expression occurs if Fez suppresses BMP signaling below a threshold level approximately 30-40% of maximal.

Discussion

The data presented here establish that Fez functions as soon as it is produced downstream of FoxQ2 to attenuate BMP signaling on one side of the animal plate, thereby maintaining the size of this neuroectodermal domain in the sea urchin embryo. This mechanism is superimposed on the well-known pathway that produces a gradient of extracellular BMP activity through the activities of its antagonists or their activating proteases (Lamb et al., 1993; Sasai et al., 1994; Piccolo et al., 1997; Lee et al., 2006; Plouhinec and De Robertis, 2009). Fez produces a significant decline of BMP2/4 activity in the outer regions of the animal plate of the early embryo along which the serotonergic neurons will subsequently develop.

The model for the mechanism and timing of Fez function is described in Figure 7. *Bmp2/4* begins to be expressed in prospective oral ectoderm of an unhatched blastula as a result of Nodal signaling, prior to the appearance of *fez* mRNA in the animal plate (Fig. 7A; Duboc et al., 2004; Materna et al., 2010). Although no pSmad1/5/8 signals were observed in this embryo, it is likely that BMP2/4 protein starts to be secreted there and to

signal at low levels because only a few hours later at hatching blastula stage low levels of pSmad1/5/8 can be detected in both aboral and anterior neurogenic ectoderm (Fig. 6B). At this time FoxQ2 and perhaps other factors induce *fez* transcription in animal plate cells (Fig. 7A). During mesenchyme blastula stages, BMP2/4 moves toward the aboral side, away from the site of *bmp2/4* transcription, possibly aided by Chordin, and establishes a gradient of activity between aboral and oral sides of the embryo (Fig. 6C, 7A; Ben-Zvi et al., 2008; Lapraz et al., 2009). The BMP activity gradient in the neurogenic ectoderm is shallow and continuous in the absence of Fez function (Fig. 6G), and probably reflects the normal morphogen gradient pattern in the extracellular space. However, in the normal embryo, the continuous gradient is perturbed at the border between neurogenic and non-neurogenic ectoderm by Fez (Fig. 6G, 7B, C), sharpening the border between the animal plate and the aboral ectoderm.

The abnormal shift of the animal plate border in Fez morphants occurs on the side where BMP signals, which reduces the size of the animal plate size in these embryos. This conclusion is supported by the observation that *foxQ2* expression is reduced where BMP2/4 signaling occurs, but Nodal signaling is prevented. The consequence is that Fez functions to stabilize the border on the aboral side along which the serotonergic neurons develop, Fez is later also expressed specifically in these neurons, although it is not required to confer neuronal identity to them. Instead it may continue to protect them from BMP signaling and/or it may be involved in promoting normal axon guidance because elongation of axons in these neurons is poorly developed in Fez morphants (Fig. 2B), as has been observed in Fez mutant mice in the olfactory bulb (Hirata et al., 2006b).

Although the data presented here indicate that Fez is involved in attenuating BMP signaling along the outer regions of the aboral animal plate ectoderm, it is still not clear how the central part of this domain is protected against BMP2/4 signaling in Fez morphants (Fig. 6). Although the pSmad1/5/8 activity is not as low as in normal embryos in this region of the animal plate, it may be below the threshold required to induce aboral, non-neurogenic ectoderm there. Alternatively, this central region is protected by a Fez-independent mechanism(s). The latter possibility is more likely because neurons differentiate in this region of animal pole ectoderm even when mis-expressed BMP2/4 generates dramatic down regulation of *foxQ2* and *fez* expression in these cells at blastula stage (Fig. 4; Yaguchi et al., 2006).

Down regulation of BMP signaling along the aboral side of the animal plate by Fez function is probably cell autonomous, although the possibility that Fez induces a

short-range signal cannot be strictly ruled out. So far, because the sequence of Fez suggests that it acts as a transcriptional repressor (Hirata et al., 2006a) rather than a Smad-interacting protein, like SIP1 (Verschueren et al., 1999; van Grunsven et al., 2003; van Grunsven et al., 2007), it is unlikely that Fez interferes directly with pSmad1/5/8 activity in intracellular region. Thus, it is possible that Fez regulates a gene(s) that is involved in pathways to maintain pSmad1/5/8 levels, such as Smad-degradation, -dephosphorylation, and/or –nucleocytoplasmic shuttling (Inman et al., 2002; Chen et al., 2006). Target genes repressed by Fez are not yet identified in the sea urchins, but, for instance, could include a gene(s) encoding proteins that promote BMP signaling or a regulatory gene(s) specifying aboral ectoderm downstream of BMP2/4 signaling. It might also support expression of several intracellular BMP signaling attenuators that have recently been identified, which include SIP1 (Nitta et al., 2004), Smurf1 (Alexandrova and Thomsen, 2006; Sapkota et al., 2007), Ski and SnoN (Deheuninck and Luo, 2009 and references cited therein). However, it is thought that the function of these intracellular factors is to pattern the neuroectoderm, not to establish it as a domain, which is what we focus on in this study. Whether they are also involved as mediators of Fez function to establish the precise border between neurogenic and non-neurogenic regions will require further investigation.

Based on previous studies, Fez family functions in several developmental steps in the central nervous systems in other animals (Shimizu and Hibi, 2009 and references cited therein), such as defining a subregion of anterior neuroetoderm (Hirata et al., 2006a) and controlling individual neural fate (Shimizu et al., 2010). With respect to molecular mechanisms, more is understood about its role in neural fate specification. In vertebrates, Fezf1 and Fezf2 control neural differentiation by suppressing Hes5 (Shimizu et al., 2010), and in flies, dFezf maintains the restricted developmental potential of intermediate neural progenitors (Weng et al., 2010). Although it has been reported that Fezf1 and Fezf2 suppress development of the caudal diencephalon in mice, and expression of *irx1* and *wnt3a*, the molecular mechanisms controlling these steps are unclear. It is also not known whether attenuation of BMP signaling is involved, as shown here in the sea urchin embryo

A combination of extrinsic and intrinsic mechanisms controls the size of the animal plate. After restriction of the animal plate to the animal pole by canonical Wnt-dependent processes, further signaling through BMP signaling can affect its size. Here we show that extracellular control of BMP signaling through antagonists is

supplemented by intracellular control within the plate itself. Similarly, Nodal signaling on the other side of the plate suppresses serotonergic neuron development and it is blocked from the animal plate by the extracellular antagonist, Lefty, and the intracellular factor, FoxQ2. What emerges from this and previous work (Yaguchi et al., 2008) is that a fascinating regulatory cassette, FoxQ2 and its downstream gene, Fez, are involved in attenuating expression of Nodal and its downstream gene, BMP2/4, sequentially to protect the neurogenic animal plate on its oral and aboral sides, respectively. These parallel mechanisms ensure that the edges of the field where neurons develop in the animal pole ectoderm are stably defined.

Acknowledgements

We thank Robert Angerer and Angerer lab members for fruitful comments on this work, Robert Burke, Yoko Nakajima, Yasunori Sasakura and David McClay for essential reagents and devices and Julius Barsi and Eric Davidson for sharing unpublished data. We thank Masato Kiyomoto and Mamoru Yamaguchi for providing the adult sea urchins and Mrs. Y. Tsuchiya, T. Sato, H, Shinagawa, and Y. Yamada, Shimoda Marine Research Center, for collecting and keeping the adult sea urchins. This work was supported, in part, by Special Coordination Funds for Promoting Science and Technology of the Ministry of Education, Culture, Sports, Science and Technology of the Japanese Government (MEXT), by Grant-in Aid for Young Scientists (Start-up No. 20870006 and B No. 21770227), and Takeda Science Foundation to S.Y., in part by the Intramural Program of the National Institutes of Health, NIDCR to L.M.A., and in part by MEXT (No. 22370023) to K.I.

References

Alexandrova, E. M. and Thomsen, G. H. (2006). Smurf1 regulates neural patterning and folding in Xenopus embryos by antagonizing the BMP/Smad1 pathway. *Dev Biol* **299**, 398-410.

Ben-Zvi, D., Shilo, B. Z., Fainsod, A. and Barkai, N. (2008). Scaling of the BMP activation gradient in Xenopus embryos. *Nature* **453**, 1205-11.

Bradham, C. A., Oikonomou, C., Kuhn, A., Core, A. B., Modell, J. W., McClay, D. R. and Poustka, A. J. (2009). Chordin is required for neural but not axial development in sea urchin embryos. *Dev Biol* **328**, 221-33.

Burke, R. D., Osborne, L., Wang, D., Murabe, N., Yaguchi, S. and Nakajima, Y. (2006). Neuron-specific expression of a synaptotagmin gene in the sea urchin Strongylocentrotus purpuratus. *J Comp Neurol* **496**, 244-51.

Chen, H. B., Shen, J., Ip, Y. T. and Xu L. (2006). Identification of phosphatases for Smad in the BMP/DPP pathway. *Gene Dev* **20**, 648-53.

De Robertis, E. M. and Kuroda, H. (2004). Dorsal-ventral patterning and neural induction in Xenopus embryos. *Annu Rev Cell Dev Biol* **20**, 285-308.

Deheuninck, J. and Luo, K. (2009). Ski and SnoN, potent negative regulators of TGF-beta signaling. *Cell Res* **19**, 47-57.

Duboc, V., Rottinger, E., Besnardeau, L. and Lepage, T. (2004). Nodal and BMP2/4 signaling organizes the oral-aboral axis of the sea urchin embryo. *Dev Cell* **6**, 397-410.

Gardner, T. S., Cantor, C. R. and Collins, J. J. (2000). Construction of a genetic toggle switch in Escherichia coli. *Nature* **403**, 339-42.

Hirata, T., Nakazawa, M., Muraoka, O., Nakayama, R., Suda, Y. and Hibi, M. (2006a). Zinc-finger genes Fez and Fez-like function in the establishment of diencephalon subdivisions. *Development* **133**, 3993-4004.

Hirata, T., Nakazawa, M., Yoshihara, S., Miyachi, H., Kitamura, K., Yoshihara, Y. and Hibi, M. (2006b). Zinc-finger gene Fez in the olfactory sensory neurons regulates development of the olfactory bulb non-cell-autonomously. *Development* **133**, 1433-43.

Inman, G. J., Nicolás, F. J. and Hill, C. S. (2002). Nucleocytoplasmic shuttling of Smads 2, 3, and 4 permits sensing of TGF-ß receptor activity. *Mol Cell* **10**, 283-94.

Kiecker, C. and Niehrs, C. (2001). A morphogen gradient of Wnt/beta-catenin signaling regulates anteroposterior neural patterning in Xenopus. *Development* **128**, 4189-4201.

Khokha, M. K., Yeh, J., Grammer, T. C. and Harland, R. M. (2005). Depletion of three BMP antagonists from Spemann's organizer leads to a catastrophic loss of dorsal structures. *Dev Cell* **8**, 401-11.

Lamb, T. M., Knecht, A. K., Smith, W. C., Stachel, S. E., Economides, A. N., Stahl, N., Yancopolous, G. D. and Harland, R. M. (1993). Neural induction by the secreted polypeptide noggin. *Science* **262**, 713-8.

Lapraz, F., Besnardeau, L. and Lepage, T. (2009). Patterning of the dorsal-ventral axis in echinoderms: insights into the evolution of the BMP-chordin signaling network. *PLoS Biol* **7**, e1000248.

Lee, H. X., Ambrosio, A. L., Reversade, B. and De Robertis, E. M. (2006). Embryonic dorsal-ventral signaling: Secreted Frizzled-related proteins as inhibitors of tolloid proteinases. *Cell* **124**, 147-159.

Logan, C. Y., Miller, J. R., Ferkowicz, M. J. and McClay, D. R. (1999). Nuclear beta-catenin is required to specify vegetal cell fates in the sea urchin embryo. *Development* **126**, 345-57.

Materna, S. C., Nam, J. and Davidson, E. H. (2010). High accuracy, high-resolution prevalence measurement for the majority of locally expressed regulatory genes in early sea urchin development. *Gene Expr Patterns* **10**, 177-84.

Minokawa, T., Rast, J. P., Arenas-Mena, C., Franco, C. B. and Davidson, E. H. (2004). Expression patterns of four different regulatory genes that function during sea urchin development. *Gene Expr Patterns* **4**, 449-56.

Nakajima, Y., Kaneko, H., Murray, G. and Burke, R. D. (2004). Divergent patterns of neural development in larval echinoids and asteroids. *Evol Dev* **6**, 95-104.

Nitta, K. R., Tanegashima, K., Takahashi, S. and Asashima, M. (2004). XSIP1 is essential for early neural gene expression and neural differentiation by suppression of BMP signaling. *Dev Biol* **275**, 258-67.

Piccolo, S., Agius, E., Lu, B., Goodman, S., Dale, L. and De Robertis, E. M. (1997). Cleavage of Chordin by Xolloid metalloprotease suggests a role for proteolytic processing in the regulation of Spemann organizer activity. *Cell* **91**, 407-16.

Plouhinec, J. L. and De Robertis, E. M. (2009). Systems biology of the self-regulating morphogenetic gradient of the Xenopus gastrula. *Cold Spring Harb Perspect Biol* **1**, a001701.

Reversade, B., Kuroda, H., Lee, H., Mays, A. and De Robertis, E. M. (2005). Depletion of Bmp2, Bmp4, Bmp7 and Spemann organizer signals induces massive brain formation in Xenopus embryos. *Development* **132**, 3381-92.

Sapkota, G., Alarcon, C., Spagnoli, F. M., Brivanlou, A. H. and Massague, J. (2007). Balancing BMP signaling through integrated inputs into the Smad1 linker. *Mol Cell* **25**, 441-54.

Sasai, Y., Lu, B., Steinbeisser, H., Geissert, D., Gont, L. K. and De Robertis, E. M. (1994). Xenopus chordin: a novel dorsalizing factor activated by organizer-specific homeobox genes. *Cell* **79**, 779-90.

Saudemont, A., Haillot, E., Mekpoh, F., Bessodes, N., Quirin, M., Lapraz, F., Duboc, V., Rottinger, E., Range, R., Oisel, A. et al. (2010). Ancestral regulatory circuits governing ectoderm patterning downstream of Nodal and BMP2/4 revealed by gene regulatory network analysis in an echinoderm. *PLoS Genet* **6**, e1001259.

Sea Urchin Genome Sequencing Consortium: Sodergren, E. Weinstock, G. M. Davidson, E. H. Cameron, R. A. Gibbs, R. A. Angerer, R. C. Angerer, L. M. Arnone, M. I. Burgess, D. R. Burke, R. D. et al. (2006). The genome of the sea urchin Strongylocentrotus purpuratus. *Science* **314**, 941-52.

Shen, Z. J., Kim, S. K., Jun, D. Y., Park, W., Kim, Y. H., Malter, J. S. and Moon, B. J. (2007). Antisense targeting of TGF-beta1 augments BMP-induced upregulation of osteopontin, type I collagen and Cbfa1 in human Saos-2 cells. *Exp Cell Res* **313**, 1415-25.

Shimizu, T. and Hibi, M. (2009). Formation and patterning of the forebrain and olfactory system by zinc-finger genes *Fezf1* and *Fezf2*. *Dev Growth Differ* **51**, 221-31.

Shimizu, T., Nakazawa, M., Kani, S., Bae, T-K., Shimizu, T., Kageyama, R. and Hibi, M. (2010). Zinc finger genes *Fezf1* and *Fezf2* control neuronal differentiation by repressing *Hes5* expression in the forebrain. *Development* **137**, 1875-85.

Spemann, H. and Mangold, H. (1924). The induction of embryonic predispositions by implantation of organizers foreign to the species. *Archiv Fur Mikroskopische Anatomie Und Entwicklungsmechanik* **100**, 599-638.

Tu, Q., Brown, C. T., Davidson, E. H. and Oliveri, P. (2006). Sea urchin Forkhead gene family: phylogeny and embryonic expression. *Dev Biol* **300**, 49-62.

van Grunsven, L. A., Michiels, C., Van de Putte, T., Nelles, L., Wuytens, G., Verschueren, K. and Huylebroeck, D. (2003). Interaction between Smad-interacting protein-1 and the corepressor C-terminal binding proteinis dispensable for transcriptional repression of E-cadherin. *J Biol Chem* **278**, 26135-26145.

van Grunsven, L. A., Taelman, V., Michiels, C., Verstappen, G., Souopgui, J., Nichane, M., Moens, E., Opdecamp, K., Vanhomwegen, J., Kricha, S., et al. (2007). XSip1 neuralizing activity involves the co-repressor CtBP and occurs through BMP dependent and independent mechanisms. *Dev Biol* **306**, 34–49.

Verschueren, K., Remacle, J. E., Collart, C., Hraft, H., Baker, B. S., Tylzanowski, P., Nelles, L., Wuytens, G., Su, M-T. Bodmer, R. et al. (1999). SIP1, a novel zinc finger/homeodomain repressor, interacts with Smad proteins and binds to 5'-CACCT sequences in candidate target genes. *J Biol Chem* **274**, 20489-98.

Wei, Z., Angerer, R. C. and Angerer, L. M. (2006). A database of mRNA expression patterns for the sea urchin embryo. *Dev Biol* **300**, 476-84.

Wei, Z., Yaguchi, J., Yaguchi, S., Angerer, R. C. and Angerer, L. M. (2009). The sea urchin animal pole domain is a Six3-dependent neurogenic patterning center. *Development* **136**, 1179-89.

Wei, Z., Angerer, R. C. and Angerer, L. M. (2011). Direct development of neurons within foregut endoderm of sea urchin embryos. *Proc Natl Acad Sci USA* **108**, 9143-47.
Weng, M., Golden, K. L. and Lee, C-Y. (2010). dFezf/Earmuff maintains the restricted developmental potential of intermediate neural progenitors in *Drosophila*. *Dev Cell* **18**, 126-35.
Wikramanayake, A. H., Huang, L. and Klein, W. H. (1998). ß-catenin is essential for patterning the maternally specified anima-vegetal axis in the sea urchin embryo. *Proc Natl Acad Sci USA* **95**, 9343-48.
Yaguchi, S., Kanoh, K., Amemiya, S. and Katow, H. (2000). Initial analysis of immunochemical cell surface properties, location and formation of the serotonergic apical ganglion in sea urchin embryos. *Dev Growth Differ* **42**, 479-88.
Yaguchi, S. and Katow, H. (2003). Expression of tryptophan 5-hydroxylase gene during sea urchin neurogenesis and role of serotonergic nervous system in larval behavior. *J Comp Neurol* **466**, 219-29.
Yaguchi, S., Yaguchi, J., Angerer, R. C. and Angerer, L. M. (2008). A Wnt-FoxQ2-nodal pathway links primary and secondary axis specification in sea urchin embryos. *Dev Cell* **14**, 97-107.
Yaguchi, S., Yaguchi, J., Angerer, R. C., Angerer, L. M. and Burke, R. D. (2010a). TGFbeta signaling positions the ciliary band and patterns neurons in the sea urchin embryo. *Dev Biol* **347**, 71-81.
Yaguchi, S., Yaguchi, J. and Burke, R. D. (2006). Specification of ectoderm restricts the size of the animal plate and patterns neurogenesis in sea urchin embryos. *Development* **133**, 2337-46.
Yaguchi, S., Yaguchi, J. and Burke, R. D. (2007). Sp-Smad2/3 mediates patterning of neurogenic ectoderm by nodal in the sea urchin embryo. *Dev Biol* **302**, 494-503.
Yaguchi, S., Yaguchi, J., Wei, Z., Shiba, K., Angerer, L. M. and Inaba, K. (2010b). ankAT-1 is a novel gene mediating the apical tuft formation in the sea urchin embryo. *Dev Biol* **348**, 67-75.

Figure legends

Figure 1. *fez* is expressed throughout the animal plate during hatched and mesenchyme blastula stages and later in the serotonergic neurons. (A) unhatched blastula of *Hemicentrotus pulcherrimus*. (B) mesenchyme blastula. (C) early gastrula. (D) mid-late gastrula. (E) prism larva. (F) pluteus stage. Asterisks in (D-F) show the individually stained cells. (G, H) *fez* is co-expressed in the animal plate with FoxQ2 at blastula stages. (I-K) In contrast, at gastrula and prism stages, *fez* is expressed in individual cells that do not express FoxQ2. (L) The pattern of later expression of *fez* is

identical to that of *tph*, which marks serotonergic neurons. Insets in I'', J'', and K'' show animal pole views of each image digitally rotated to show the asymmetry of *foxQ2* and *fez* patterns along the secondary axis (o and ab show oral and aboral side, respectively). (M-O) *fez* expression depends on FoxQ2. (M) *fez* is expressed in the animal plate region of control (gly; glycerol-injected) mesenchyme blastula-stage embryos (black arrowhead). (N) FoxQ2 morphant (FoxQ2-MO) lacks *fez* expression (white arrowhead). (O) Quantitative PCR (QPCR) shows *fez* expression depends on FoxQ2 at early stages (20hr, hatching-mesenchyme blastula; 26hr, gastrula), but not at a later stage (48hr; pluteus). X axis= time after fertilization. Y axis = ΔΔCt, the cycle differences after normalization for load between experimental and control embryos (one negative cycle difference means that the mRNA concentration is reduced two fold). QPCR was performed by the following the method described in Yaguchi et al. (2010b). Bar in (A) = 20 μm.

Figure 2. The animal plate size is smaller in Fez morphants (Fez-MO). (A-C) Serotonergic neurons and synaptotagminB (synB)-positive neurons in 72-hour control embryos (A), in 72-hour Fez morphant (B) and in 72-hour Fez-mRNA injected embryo (C). (D, F) SynB-neurons and Nk2.1, prism stage in control (D), and in Fez morphant (Fez-MO; F). All of syn-B positive neurons at animal plate are serotonergic at this stage. *hbn* expression pattern in control (E), and in Fez morphant (G). Lines in (D), and (F) show the distance between two neurons. Brackets in (E) and (G) show the size of neurogenic ectoderm. Bars in (A) and (D) = 20 μm, and refer to panels (A-C) and (D-G), respectively.

Figure 3. Fez is not involved in the differentiation of serotonergic neurons. (A) Experimental flow to investigate whether Fez functions in neural differentiation. (B-G) Serotonergic neurons and synaptotagminB (synB)-positive neurons, in pluteus larvae subjected to the following treatments: (B), DAPT (C), Fez morpholino (D), DAPT and Fez morpholino (E), Fez mRNA injection (F), and DAPT and Fez mRNA injection (G). The anterior regions of embryos indicated by the dashed square in the middle panels are magnified in the right panels; ,a double arrow shows the direction of oral (o)-aboral (ab) axis. Bar in (B) = 20 μm.

Figure 4. Fez attenuates BMP signaling, which antagonizes neurogenic ectoderm development. (A-F) Fez is required to maintain the size of the region expressing *foxQ2* and *nk2.1*. (A) *foxQ2* mRNA, control hatching blastula (HBL). (B) *foxQ2* mRNA, control mesenchyme blastula (MBL). (C) *nk2.1* mRNA, control, MBL. (D) *foxQ2* mRNA, Fez morphant, HBL. (E) *foxQ2* mRNA, Fez morphant, MBL. (F) *nk2.1* mRNA, Fez morphant, MBL. (G-J) BMP2/4 does not suppress *foxQ2* or *fez* expression outside the animal plate of MBL. (G) *foxQ2* mRNA, control. (H) *fez* mRNA, control. (I) *foxQ2* mRNA, BMP2/4 morphant. (J) *fez* mRNA, BMP2/4 morphant. (K, L) Mis-expressed BMP2/4 can suppress *foxQ2* (K) and *fez* (L) expressions. (M-P) The *foxQ2* expression domain is reduced in Fez morphants, but not in double Fez/BMP2/4 morphant MBL (M) control and (N) Fez morphant; BMP2/4 morphant (O) and (P) BMP2/4-Fez double morphant. Double-headed arrows in (B, E, M-P) show *foxQ2*-positive animal plate. Arrowhead and double arrowheads in (K) and (L) show that in embryos over-expressing BMP2/4, both FoxQ2 and fez expression is strongly reduced. Bar in (A) and (O) = 20 μm, and refer to panels (A-F, I-N) and (O-R), respectively.

Figure 5. BMP2/4, not Nodal, reduces the neurogenic ectoderm size in the absence of Fez in mesenchyme blastulae (MBL). (A) Protocol producing control experimental embryos in which Nodal signaling is restricted to one half of the embryo by injection of activated Smad2/3 mRNA into one of the two-cell embryo blastomeres. (B) *foxQ2* mRNA, (B') *myc* mRNA, (B'') Merged image of (B) and (B'). Merged and magnified image of square region in (B'') is shown in the right panel with DAPI. (C) Drawing showing the ectodermal partitioning of experimental control embryo. Green, blue, and magenta show oral, aboral, and animal plate ectoderm, respectively. *bmp2/4*, transcribed in oral ectoderm in response to activated Smad2/3, produces BMP2/4 which diffuses to the aboral side. (D) Protocol producing experimental embryos lacking Fez function. (E) *foxQ2* (E'), *myc* (E''), Merged image of (E) and (E'), and the merged and magnified image of square region in (E'') with DAPI is shown in the right panel. (F) Drawing showing the ectodermal partitioning of the experimental embryo in which Fez translation is blocked, which causes reduction of the animal plate on the side of the embryo where BMP2/4 signals. (G) Protocol producing experimental embryos lacking BMP2/4 function. (H) *foxQ2*, (H') *myc*, (H'') Merged image of (H) and (H'), and the merged and magnified image of square region in (H'') is shown in the right panel with

DAPI. (I) Drawing showing the ectodermal partitioning of experimental embryo, in which BMP2/4 translation is blocked. (J) Protocol producing experimental embryos lacking BMP2/4 and Fez function. (K) *foxQ2*, (K') *myc*, (K'') Merged image of (K) and (K'), and the merged and magnified image of square region in (K'') with DAPI is shown in the right panel. (L) Drawing showing the ectodermal partitioning of experimental embryo, in which BMP2/4 and Fez translation is blocked. (M) Histograms showing the number of *foxQ2*-positive cells in *myc*- and Nodal signaling-negative side of experimental embryos. Counts were made from specimen from two independent batches. Bar in (B) = 20 μm. Arrowhead in the right panel of (E'') shows the site where FoxQ2 expression is lost.

Figure 6. BMP2/4 diffuses over the animal plate region and builds an activity gradient at mesenchyme blastula stage. Accumulation of pSmad1/5/8 in the ectoderm during blastula stages. (A, B, C) Phospho-Smad1/5/8 (pSmad1/5/8); (A', B', C') FoxQ2; (A'', B'', C'') Merged image (A''', B''', C''') Merged image with DAPI nuclear stain, and a square in A''', B''' and C''' indicates the magnified region shown in A-A'', B-B'', and C-C'', respectively. (A) unhatched blastula. (B) hatching blastula. (C) mesenchyme blastula. (D, E) The accumulation of pSmad1/5/8 in the animal plate region is altered in Fez morphants at mesenchyme blastula stage. (D, E) pSmad1/5/8; (D', E') FoxQ2, which marks the animal plate; (D'', E'') merged image; (D''', E''') merged image with DAPI nuclear staining, and a square in D''' and E''' indicates the magnified region shown in D-D'' and E-E'', respectively. (F) The intensities of fluorescent signals in nuclei for pSmad1/5/8 and FoxQ2 were measured with ImageJ for each cell along a line extending outward from the center of the animal plate to the center of the aboral side as illustrated (white dots). Some dark regions unlabeled by either FoxQ2 or pSmad1/5/8 antibodies are ectoderm folds that occur as a result of embryo processing procedures. We selected embryos in which there are no folds observed along the line to avoid inaccurate measurements. (G) Relative fluorescent signal intensities of pSmad1/5/8 and FoxQ2 in the animal plate/aboral ectoderm region in control (upper panel) and Fez morphants (lower panel). The data were normalized in each individual, and then averaged using 3-4 embryos per mating pair. Data collected from three independent batches are shown by individual line, and pSmad1/5/8 and FoxQ2 signals are shown by solid green and dotted magenta lines, respectively. Bars in (A''') and (D''') = 20 μm, and refer to panels (A-C) and (D, E), respectively. Asterisks in (D, E) show the center of FoxQ2 region.

Figure 7. Model for the timing and location of Fez suppression of BMP signaling in the sea urchin embryo. (A) BMP2/4 protein theoretically synthesized in the future oral ectoderm of unhatched blastula diffuses throughout the ectoderm including the animal plate. The highest activity of BMP2/4 is observed on the aboral side at mesenchyme blastula stage. *fez*/Fez begins to be expressed in the neurogenic animal plate at hatching blastula stage. (B) FoxQ2 appears first in the animal plate before BMP signaling. Fez is induced by FoxQ2 and reaches levels sufficient to attenuate BMP at the outer edges of the animal plate so that BMP cannot inhibit FoxQ2 there. (C) The relationship between pSmad1/5/8 activity and the size of animal plate with/without Fez function. In normal embryos with Fez function (upper panel), the activity of pSmad1/5/8 is dramatically decreased at the border between Fez-negative and -positive region to a level that preserves FoxQ2 expression and the animal plate. In Fez morphants (lower panel), the gradient of pSmad1/5/8 is continuous from the aboral ectoderm to the animal pole and the abnormally high levels of pSmad1/5/8 in the periphery of the animal plate prevent expression of FoxQ2 and differentiation of the animal plate.

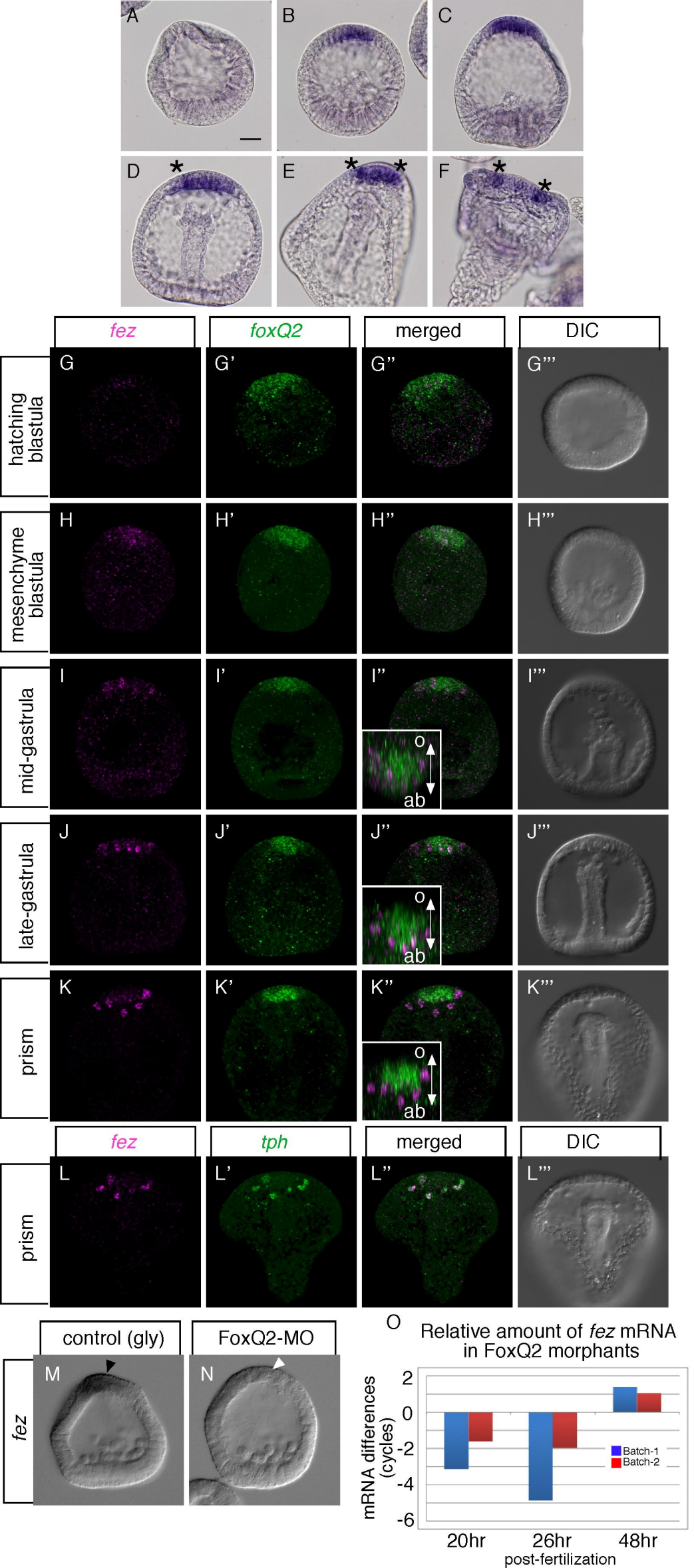
A
B
C
D
E
F
fez
foxQ2
merged
DIC
hatching blastula
mesenchyme blastula
mid-gastrula
late-gastrula
prism
G
G'
G''
G'''
H
H'
H''
H'''
I
I'
I''
I'''
J
J'
J''
J'''
K
K'
K''
K'''
o
ab
fez
tph
merged
DIC
prism
L
L'
L''
L'''
control (gly)
FoxQ2-MO
fez
M
N
O
Relative amount of fez mRNA in FoxQ2 morphants
mRNA differences (cycles)
2
0
-2
-4
-6
Batch-1
Batch-2
20hr
26hr
48hr
post-fertilization

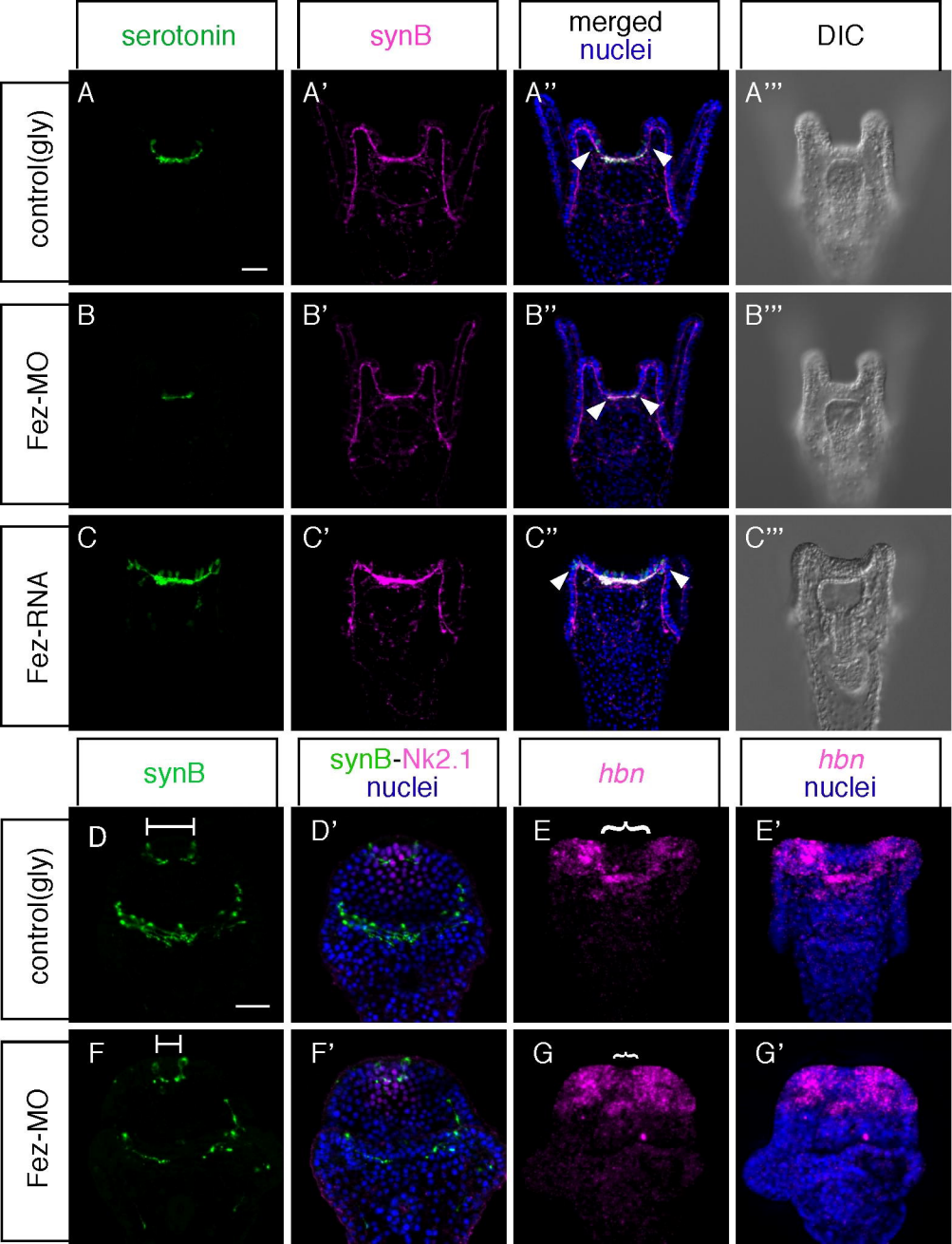
serotonin
synB
merged
nuclei
DIC
control(gly)
Fez-MO
Fez-RNA
A
A'
A''
A'''
B
B'
B''
B'''
C
C'
C''
C'''
synB
synB-Nk2.1
nuclei
hbn
hbn
nuclei
D
D'
E
E'
F
F'
G
G'

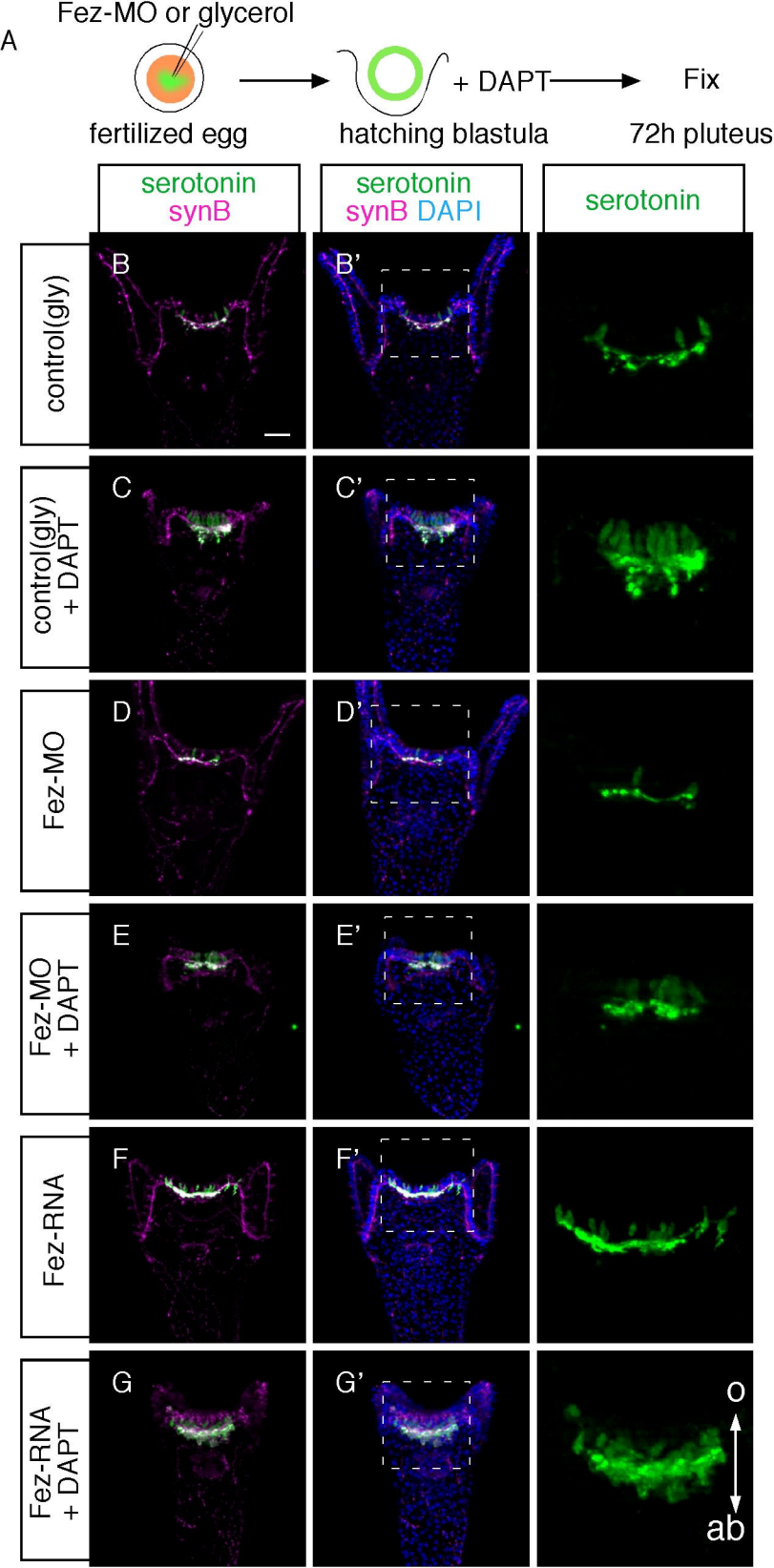
A
Fez-MO or glycerol
fertilized egg
+ DAPT
hatching blastula
Fix
72h pluteus
serotonin
synB
serotonin
synB DAPI
serotonin
control(gly)
control(gly)
+ DAPT
Fez-MO
Fez-MO
+ DAPT
Fez-RNA
Fez-RNA
+ DAPT
B
B'
C
C'
D
D'
E
E'
F
F'
G
G'
o
ab

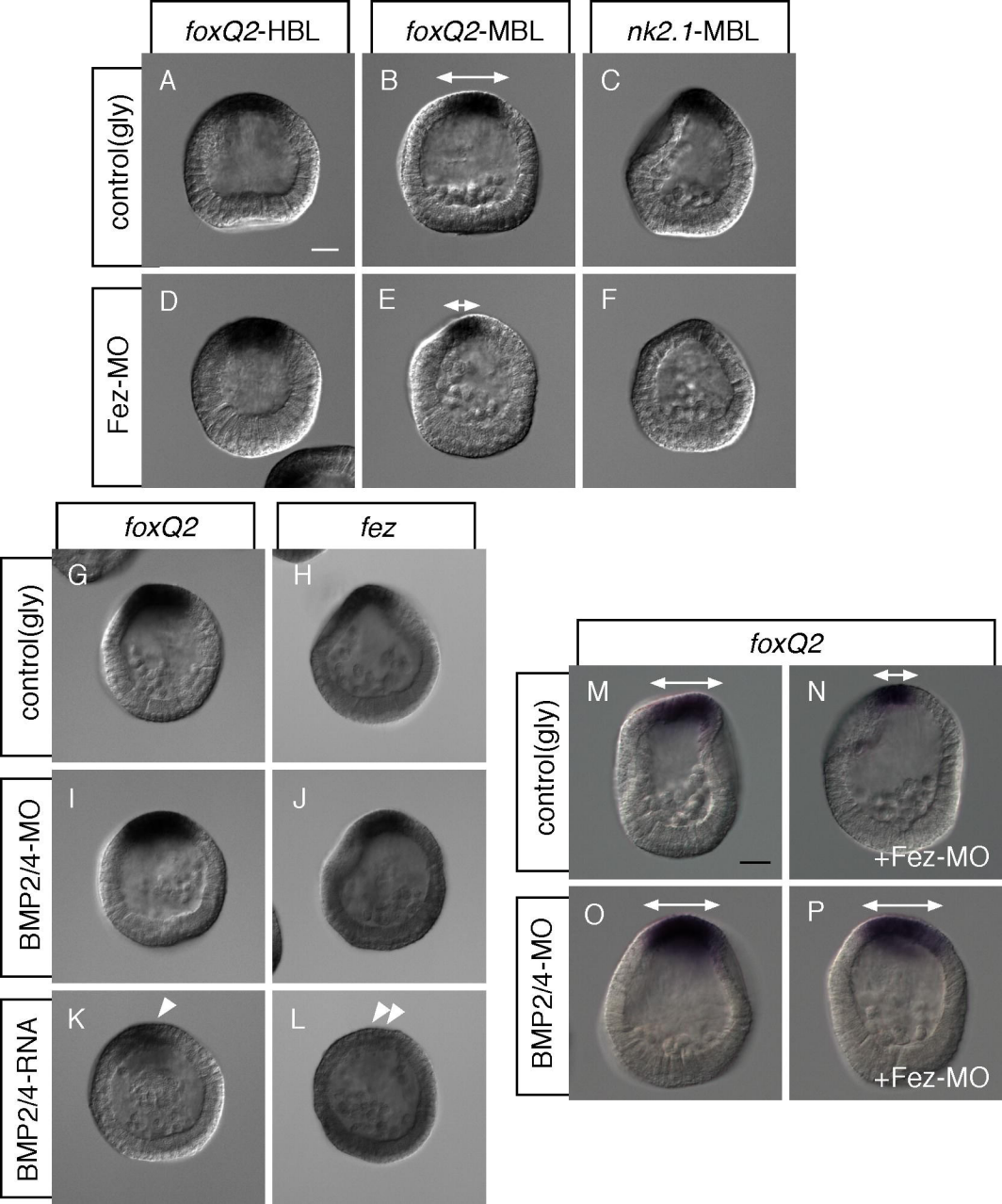
foxQ2-HBL
foxQ2-MBL
nk2.1-MBL
control(gly)
Fez-MO
A
B
C
D
E
F
foxQ2
fez
control(gly)
BMP2/4-MO
BMP2/4-RNA
G
H
I
J
K
L
foxQ2
control(gly)
BMP2/4-MO
M
N
O
P
+Fez-MO
+Fez-MO

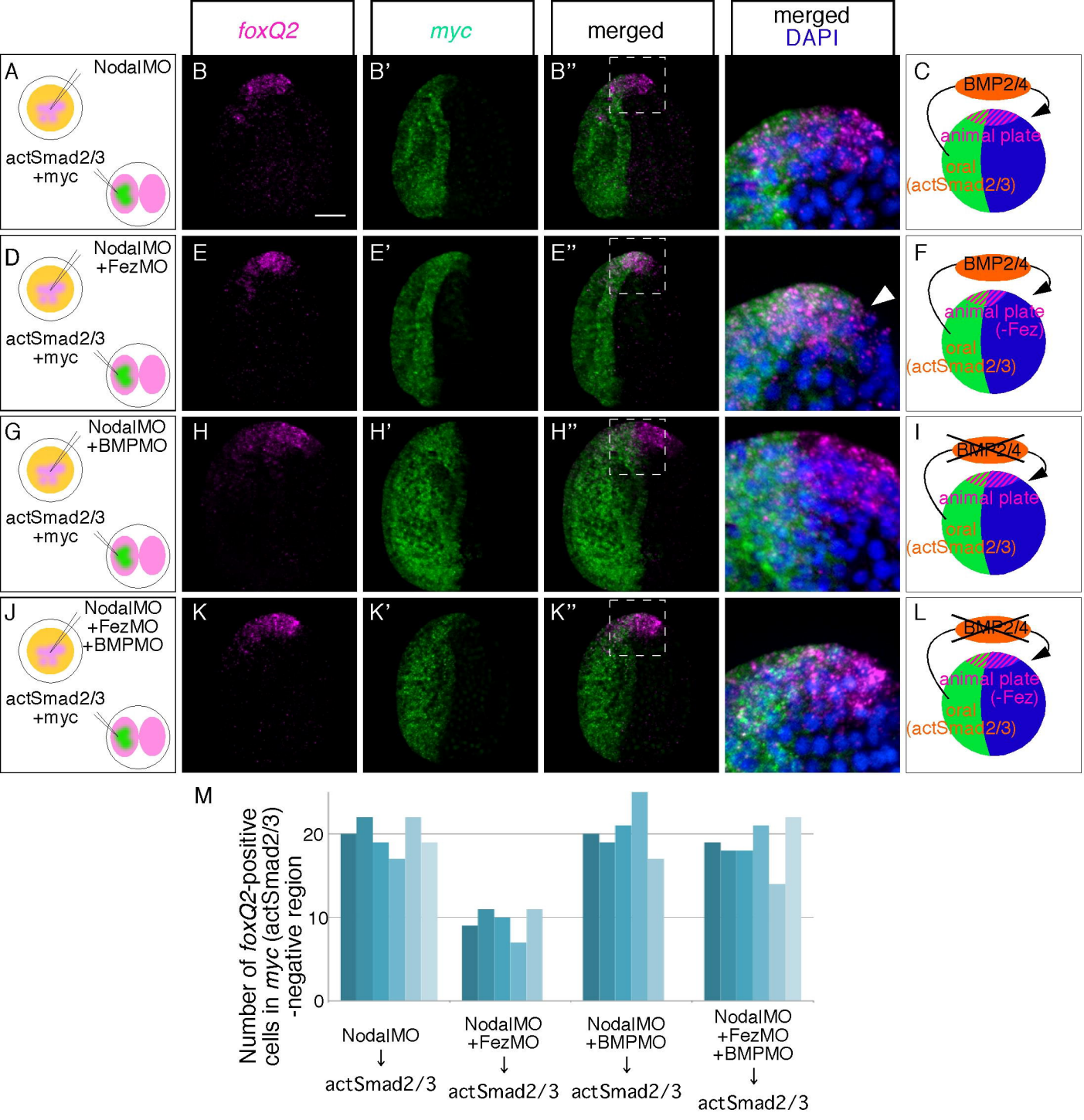
foxQ2
myc
merged
merged
DAPI
A
NodalMO
actSmad2/3
+myc
B
B'
B''
C
BMP2/4
animal plate
oral
(actSmad2/3)
D
NodalMO
+FezMO
actSmad2/3
+myc
E
E'
E''
F
BMP2/4
animal plate
(-Fez)
oral
(actSmad2/3)
G
NodalMO
+BMPMO
actSmad2/3
+myc
H
H'
H''
I
BMP2/4
animal plate
oral
(actSmad2/3)
J
NodalMO
+FezMO
+BMPMO
actSmad2/3
+myc
K
K'
K''
L
BMP2/4
animal plate
(-Fez)
oral
(actSmad2/3)
M
Number of foxQ2-positive
cells in myc (actSmad2/3)
-negative region
20
10
0
NodalMO
↓
actSmad2/3
NodalMO
+FezMO
↓
actSmad2/3
NodalMO
+BMPMO
↓
actSmad2/3
NodalMO
+FezMO
+BMPMO
↓
actSmad2/3

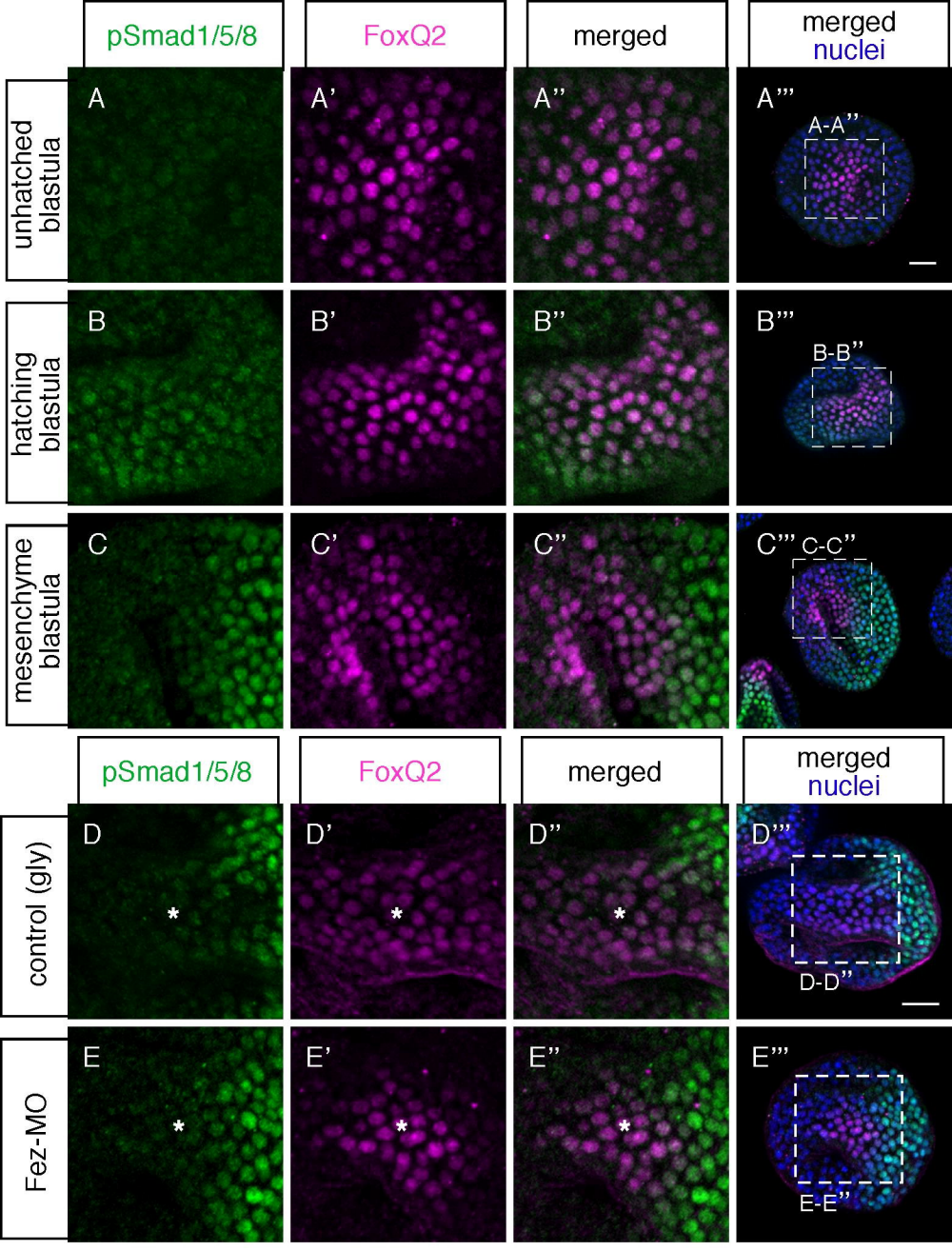

F

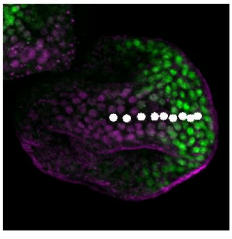

animal pole view

G

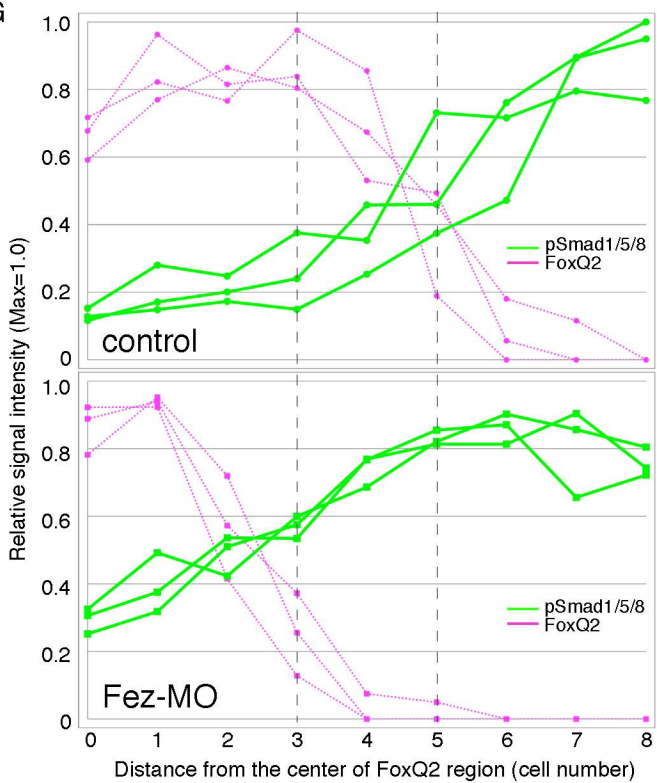

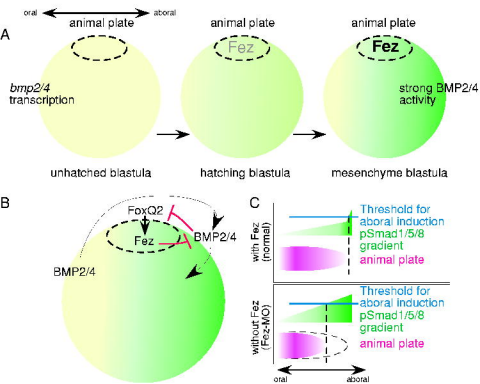
A
oral
aboral
animal plate
animal plate
animal plate
Fez
Fez
bmp2/4
transcription
strong BMP2/4
activity
unhatched blastula
hatching blastula
mesenchyme blastula
B
FoxQ2
Fez
BMP2/4
BMP2/4
C
with Fez
(normal)
Threshold for
aboral induction
pSmad1/5/8
gradient
animal plate
without Fez
(Fez-MO)
Threshold for
aboral induction
pSmad1/5/8
gradient
animal plate
oral
aboral